Journal of Alloys and Compounds 495 (2010) 650–654

Contents lists available at ScienceDirect

Journal of Alloys and Compounds

journal homepage: www.elsevier.com/locate/jallcom

Hydrogen desorption in nanocrystalline MgH_2 thin films at room temperature

J.R. Ares [a,*], F. Leardini [a], P. Díaz-Chao [a], J. Bodega [a], D.W. Koon [b,*], I.J. Ferrer [a], J.F. Fernández [a], C. Sánchez [a]

[a] Dpto. de Física de Materiales, Facultad de Ciencias, Universidad Autónoma de Madrid, Cantoblanco, 28049, Madrid, Spain
[b] Physics Department, St Lawrence University, Canton, NY, 13617, USA

ARTICLE INFO

Article history:
Received 31 July 2008
Received in revised form 14 October 2009
Accepted 15 October 2009
Available online 24 October 2009

Keywords:
Hydrogen absorbing materials
Thin films
Vapour deposition
Kinetics
Thermal analysis

ABSTRACT

Hydrogen desorption process of Pd-capped magnesium hydride thin films of different thicknesses was investigated. Decomposition of magnesium hydride into magnesium under air exposure is observed in all investigated films. During decomposition no novel crystalline phases are detected. Desorption process was qualitatively analysed and it was concluded that is thermodynamically driven controlled by a nucleation and growth or by an interphase controlled mechanism. Moreover, H-kinetics investigation of desorption process was carried out by thermal desorption spectroscopy. Decomposition of MgH_2 films occurs at $T_d \sim 148\,^{\circ}C$ and the process seems to be controlled by a bidimensional interphase mechanism with an activation energy of 135 ± 20 kJ/mol H_2. No significant influence of thickness and crystallite size on desorption temperature is observed and obtained activation energy is similar to that of milled bulk magnesium.

1. Introduction

Magnesium hydride (MgH_2) is an archetypical system used to investigate hydrogen storage for transport purposes [1,2]. However, up to now, its utilization has been prevented due to its poorly kinetics and high stability (76 kJ/mol H_2). In order to overcome those drawbacks, research is starting to be focused on Mg-nanostructures i.e. nanowires and nanoparticles [3–5] because of the better predicted thermodynamic and kinetics properties [6] than those exhibited by bulk-Mg. Among those nanostructures, capped Pd magnesium thin films seem to be an excellent tool to investigate those predicted improvements and other related phenomena such as influence of microstructure or/and additives on magnesium hydride properties in a better controlled way. Moreover, magnesium thin films could also be used in other hydrogen related systems such as switchable mirrors [7] and hydrogen sensors [8].

However, despite H-absorption process in capped palladium magnesium film is, basically, well understood [9], H-desorption process shows much more discrepancies within the scarce previous literature. For instance, the desorption temperature of magnesium hydride thin films (T_d) varies into a wide range from 80 °C to 250 °C [10–13], the influence of structural parameters (for instance the crystallite size) on desorption temperature is revealed contradictory in different works [10,12] and, finally, the H-desorption mechanism has not been deeply investigated [13].

Those discrepancies are complex to explain due to different reasons, i.e. scarce literature, different preparation and experimental conditions used, the influence of oxides, hydroxides on kinetics and thermodynamic properties (much more important than those in bulk [14]). Therefore, previously to further investigations, it is needed to clarify the causes of those discrepancies and afterwards, the influence of structural and morphological parameters (thickness, crystallite size, strain, etc.) on H-desorption mechanism.

In this paper, we provide a first approach about the desorption process of magnesium hydride films with different thicknesses. We have found that films desorb spontaneously hydrogen when exposed to air. Desorption process has been characterized by different techniques (GRXD, RBS, TDS, etc.). A qualitatively explanation to the desorption mechanism is discussed as well as the main reasons of the discrepancies of previous data.

2. Experimental

Magnesium films of nominal thicknesses of 300 nm and 100 nm respectively, were prepared by e-beam evaporation at RT on aluminium and glass substrates under a background pressure of 10^{-6} mbar. In order to protect against oxidation and facilitate dissociation/recombination process of H_2 [15] Mg-films were capped by a palladium layer of 10 nm. Evaporation rates of 1 nm/s and 0.02 nm/s were used in magnesium and palladium, respectively. Nominal thicknesses were determined "in situ" by a quartz microbalance.

Structural characterization of films was carried out by glancing angle X-ray diffraction (Panalytical X'pert Pro diffractometer) with Cu Kα radiation at an

* Corresponding authors. Tel.: +34 914974777; fax: +34 914978579.
E-mail address: joser.ares@uam.es (J.R. Ares).

0925-8388/$ – see front matter © 2009 Elsevier B.V. All rights reserved.
doi:10.1016/j.jallcom.2009.10.110

incidence angle of 1.7°. "Ex situ" thickness and roughness of films were obtained by a Sloan Dektak IIA Profilometer (accuracy ±1 nm).

Morphological characterization was carried out by SEM-FEG mod. FEI XL-30. Compositional depth profile was investigated by Rutherford Backscattering Spectroscopy (RBS) at 5 MeV Cocktroft–Walton tandentron accelerator. He^+ ions were used. Analysis of the results was performed with RBX software [16].

Films were hydrogenated into a Sievert type apparatus at 1 MPa of hydrogen during 20 h at 100 °C. The desorption process was performed by thermal desorption spectroscopy (TDS) measurements with a quadrupole mass spectrometer (QMS 200 Balzers) under an Argon flux of 56 sccm [17]. Films were heated with a heating rate of 20 °C/min. Calibration experiments have been performed to determine the detection sensitivity of the TDS system (σ) for H_2. This sensitivity relates the H_2 flow evolved from the samples (F_{H_2}) to the mass spectrometric ionic signal i_2 is:

$$F_{H_2} = \sigma(i_2 - i_2^0) \quad (1)$$

where i_2^0 is the ionic signal corresponding to the residual H_2 atmosphere in the experimental system. σ values have been obtained by using MgH_2 powders (Alfa Aesar, 95%) and relating the time integrals of the ionic signals to the H_2 mol number desorbed from the samples (determined by gravimetric measurements). The obtained sensitivity is $\sigma = 22{,}900 \pm 500$ mol/C.

3. Results and discussion

3.1. Mg–Pd films characterization

Fig. 1a and b shows the X-ray diffraction pattern as well as SEM micrographs of the as-prepared Pd capped-Mg films with measured thicknesses of 320 ± 20 nm and 110 ± 10 nm, respectively. Both films show an average roughness of 3 ± 0.5 nm. Magnesium and palladium phases are detected by XRD measurements in all investigated films. No other crystalline phases are detected.

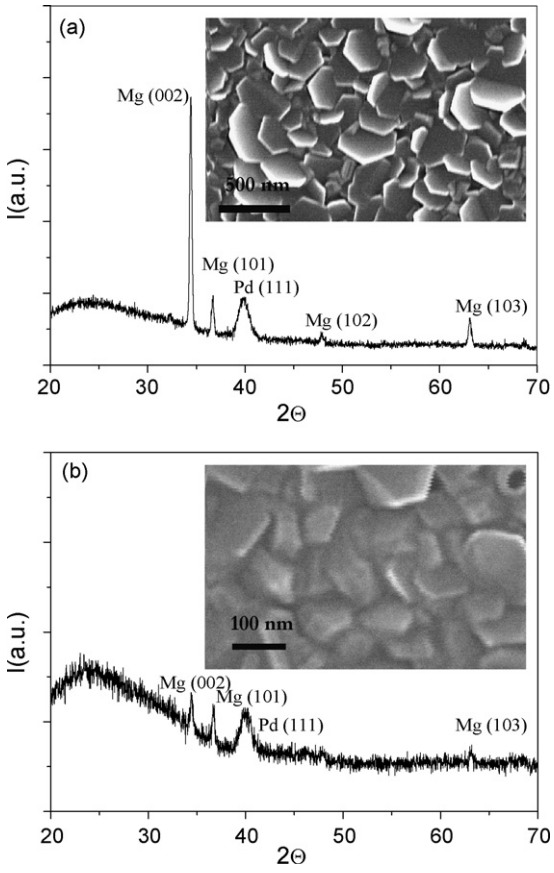

Fig. 1. (a) X-ray diffraction pattern of magnesium film with nominal thickness of 300 nm. Inset shows a micrograph of the film surface obtained by SEM. (b) X-ray diffraction pattern of magnesium film with nominal thickness of 100 nm. Inset shows a SEM micrograph of the film surface.

A preferred orientation of magnesium crystallites along (0 0 2) plane in the thick films (nominal thickness of 300 nm) is observed in the XRD pattern (Fig. 1a). The orientation along the basal plane is also observed at the SEM micrograph in a clear way (crystallites exhibit a characteristic hexagonal shape parallel to the surface). However, concerning thinner films (nominal thickness of 100 nm), they exhibit less preferred orientation as X-ray diffraction pattern and the SEM micrograph reveal in Fig. 1b. Columnar growing has been previously reported in magnesium films deposited with other evaporation methods as sputtering [18] indicating that this sort of growing along (0 0 2) plane is energetically more favourable than those along other directions.

As concerns microstructure, magnesium crystallite sizes obtained by Scherrer formulae [19] agree reasonable well to those observed by SEM. A significant diminution of magnesium crystallite size (from 300 nm to 120 nm) when magnesium film thicknesses is decreased from 320 nm to 110 nm is observed. As regards palladium crystallite size, it remains constant (8 ± 3 nm).

3.2. Dehydriding process at room temperature

Once hydrogenated, magnesium films increase their thickness due to hydrogenation process, i.e. thicker films increase from 320 ± 20 nm to 380 ± 20 nm and thinner films from 110 ± 20 nm to 135 ± 15 nm. Increase is related to cell volume expansion of Mg to become MgH_2 (a cell volume ratio (V_{MgH_2}/V_{Mg}) of ~1.32 is expected). Moreover, it was observed that films desorbed spontaneously hydrogen at RT under air. This result confirms the previous qualitative observations reported by Checchetto et al. [13]. TDS measurements were carried out to quantify the amount of hydrogen remaining in films after exposing different times under air. Fig. 2a and b shows the influence of exposure time on hydrogen content in films with different thickness. It is observed that films desorb hydrogen. For instance, whereas the thinner MgH_2-films are completely desorbed in 2000 min, the thicker ones just desorb around 40% of its initial H-capacity at that time.

H-desorption process of magnesium hydride films at RT is clearly related to decomposition of MgH_2 into Mg as revealed by XRD. XRD patterns of the hydrided samples performed at different exposure times in air are shown in Figs. 3 and 4. As regards thick films (Fig. 3a), after a short exposure to air MgH_2, Mg and Pd crystalline phases are already detected. No other crystalline phases are detected. An initial crystallite size ~80 ± 20 nm of MgH_2 is obtained by Scherrer formulae [19]. Longer exposure times lead to a decrease of MgH_2 diffraction peak (Fig. 3b and c) whereas magnesium crystalline phase increases. It is remarkable that magnesium formed after decomposition exhibits similar preferred orientation (along 0 0 2 plane) and crystallite size as the as-growth magnesium films. Similar behaviour is observed at thinner films, i.e. decomposition from MgH_2 into Mg (Fig. 4a and b), with the difference that initial crystallite size of MgH_2 is smaller (30 ± 10 nm) than that of thicker hydrided films.

Moreover, after H-desorption, bumps on the surface of the films are detected in both samples. Figs. 5 and 6 show the SEM pictures of the films after hydrogen desorption. Those bumps have already been observed by other authors [12] and they are usually attributed to strain effects because of expansion/contraction of the lattice during the H-absorption/desorption process. These results agree with our data because those bumps are more numerous in thinner films (Figs. 5 and 6) than thicker ones suggesting that could be related to strain effects induced by substrate on films. It is remarkable, however, that palladium layer remains practically identical after H-desorption process. Palladium crystallite size remains constant and, besides, RBS measurements do not show any appreciable change on palladium layer as Figs. 7a and b show. Only a small increase of oxygen amount (from ~5% to ~12%) is detected

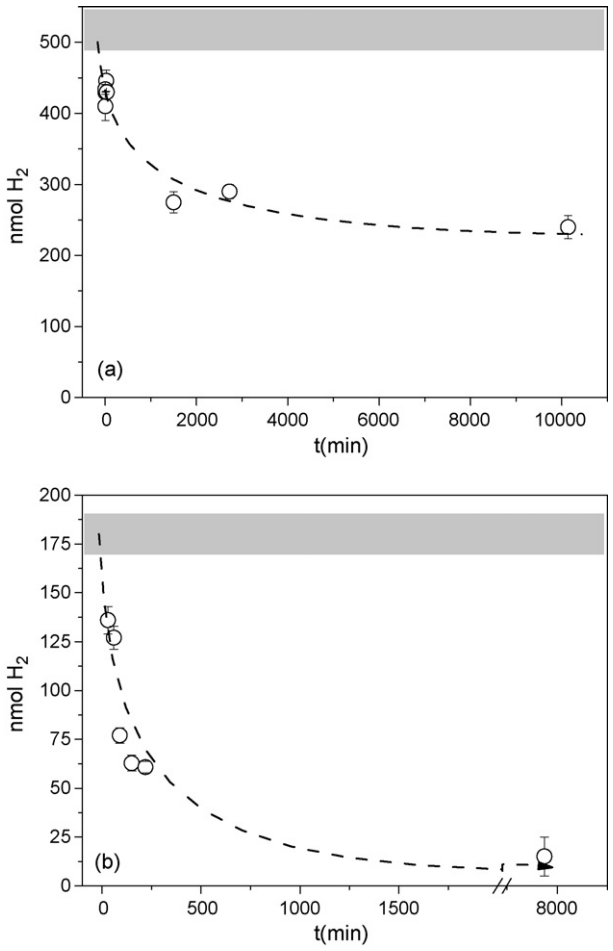

Fig. 2. Time evolution of hydrogen content in hydrogenated magnesium films under air exposure with nominal thickness of (a) 300 nm and (b) 100 nm. Grey regions correspond to H-amount related to a complete MgH_2 layer.

into magnesium layer compared to non-hydrogenate films. Moreover, RBS measurements indicate that films density is lower than bulk density (i.e. magnesium layer densities is $\sim$1.48 g/cm^3) as it is expected due to great amount of defects usually exhibited by thin films.

The RT decomposition of MgH_2 thin films observed in Fig. 2a and b imply that this process is not so drastically kinetically limited as occurs in bulk. Magnesium hydride decomposition is thermodynamically favourable because partial hydrogen pressure at RT in air is lower ($\sim 5 \times 10^{-7}$ mb) [20] than the equilibrium pressure of MgH_2 ($\sim 10^{-6}$ mb) i.e. magnesium hydride is unstable in air and a thermodynamically driven decomposition is expected.

As occurs in bulk MgH_2, the desorption mechanism of magnesium hydride films could be controlled by different processes: hydrogen recombination on the surface, hydrogen diffusion and/or nucleation and growth of α-Mg phase. In principle, surface effects may be disregard because magnesium surface is covered by a palladium layer. Palladium seems to improve hydrogen recombination and protect the surface against oxidation [15,21]. Moreover, in our case, palladium layer seems practically to be unaltered during the desorption process as RBS and XRD measurements show (due to low temperatures used) which should keep its catalytic properties unaltered.

Concerning hydrogen diffusion, we could expect that hydrogen diffusion into α-Mg could be the rate limiting mechanism. However, the calculated value of the diffusion coefficient (apply-

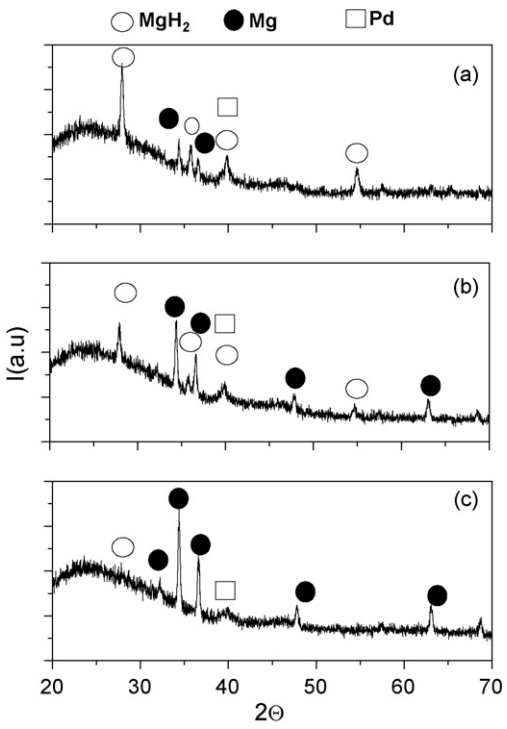

Fig. 3. X-ray diffraction pattern of hydrogenated magnesium film after air exposure of (a) 300 min (b) 1800 min and (c) 12,000 min. Nominal thickness of the film is 300 nm.

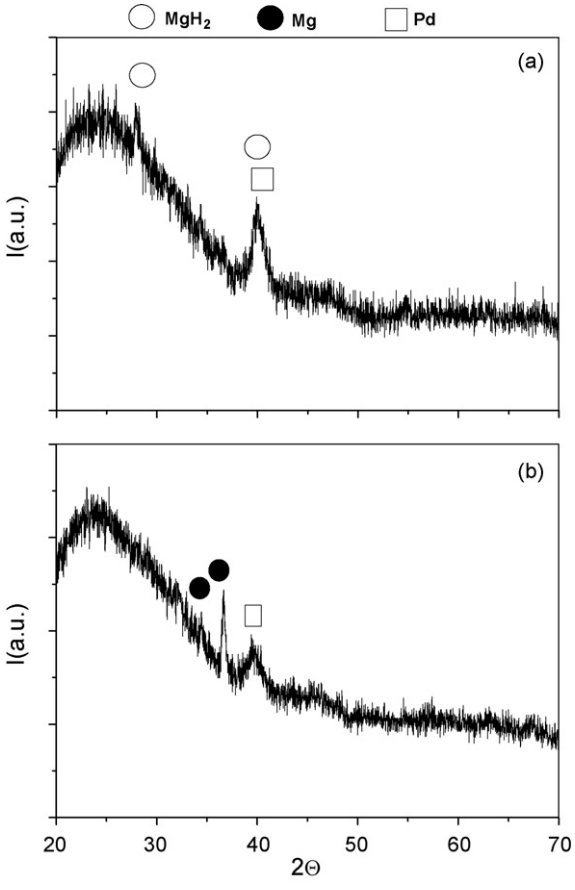

Fig. 4. X-ray diffraction pattern of magnesium hydride film after air exposure of (a) 200 min and (b) 6000 min. Nominal thickness of the film is 100 nm.

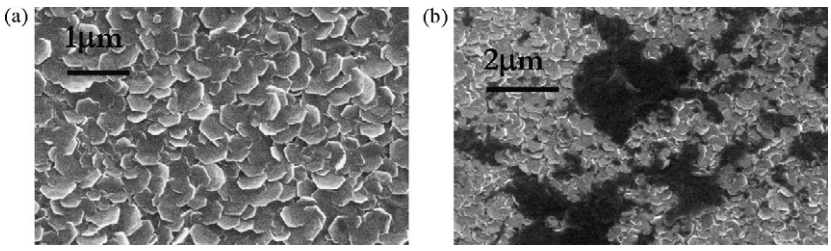

Fig. 5. (a) SEM micrograph of desorbed magnesium film with nominal thickness of 300 nm and (b) SEM image of holes at the surface.

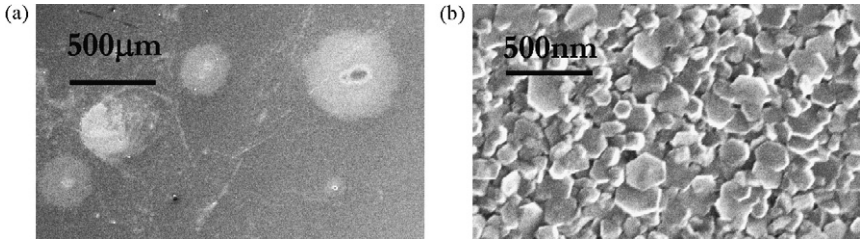

Fig. 6. (a) SEM micrograph of desorbed magnesium film with nominal thickness of 100 nm and (b) SEM image of bumps at the surface.

ing the 1D diffusion equation ($x = \sqrt{Dt}$)), at room temperature ($D = 2 \times 10^{-12}$ cm^2/s) is much lower that those reported in the literature [22,23]. Therefore, the rate limiting step should be controlled by interphase or by nucleation and growth mechanism as occurs in bulk magnesium hydride [24].

3.3. Thermal desorption spectroscopy measurements

In order to get more information about the desorption process such as activation energies, TDS measurements were done after being hydrogenated to avoid a non-controlled H-desorption

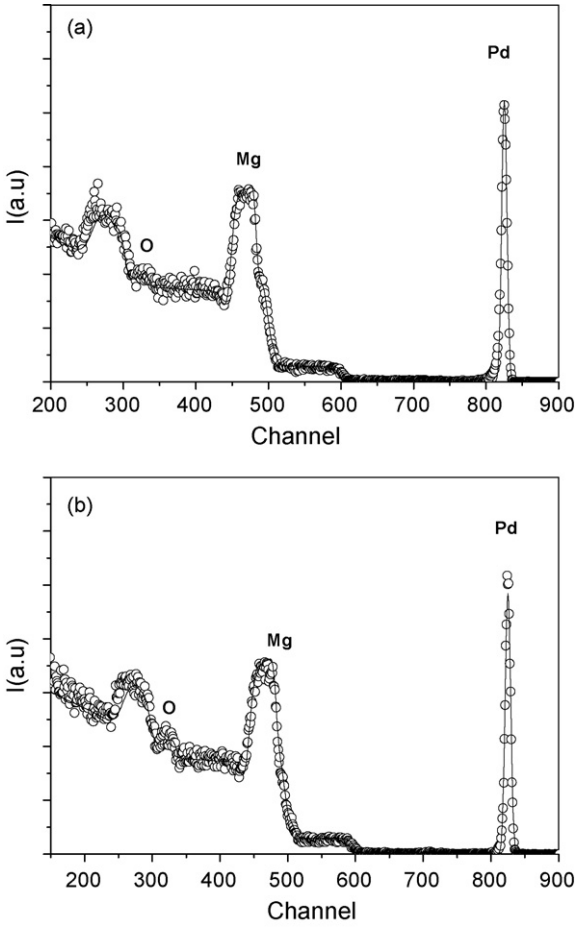

Fig. 7. RBS measurements of a magnesium film with nominal thickness of 300 nm (a) as-prepared (b) after absorption/desorption cycle.

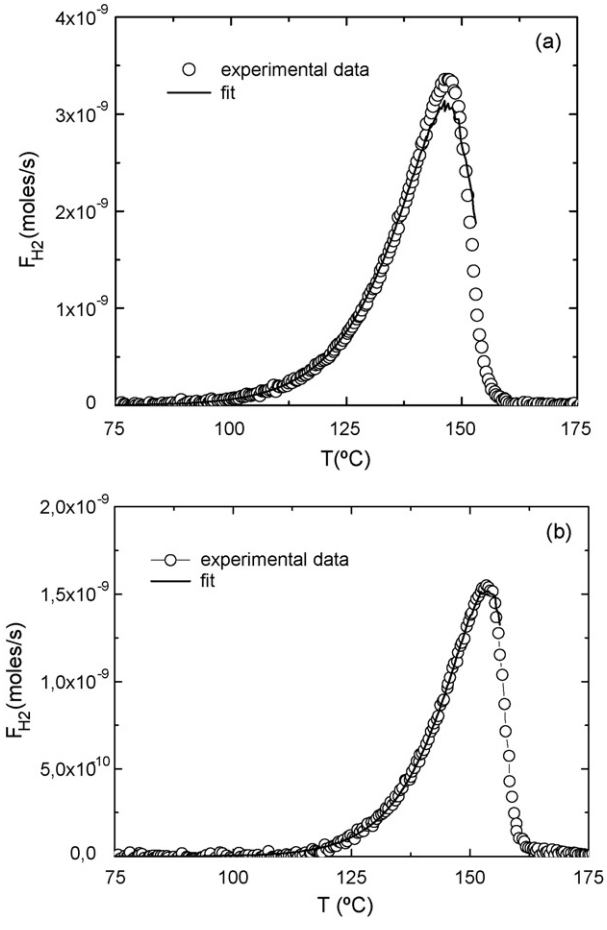

Fig. 8. Thermal desorption spectra of hydrogenated magnesium films with nominal thicknesses of (a) 300 nm and (b) 100 nm. Best fit to both curves correspond to a 2D-interphase control mechanism given by Eq. (2).

process. Fig. 8a and b shows the thermal desorption spectra of films with different thicknesses. No other species but hydrogen are detected. Films of different thicknesses exhibit only one desorption peak with similar desorption temperature ($148 \pm 5\,^{\circ}C$). Previous literature shows desorption process occurs with more than one peaks which is attributed to different causes (hydrogen in Pd–Mg interface, hydrogen in grain boundaries, etc.) and a wide range of desorption temperatures is observed [10]. This influence could be due to H-desorption produced in hydrides films which has not been considered.

By solid-state reaction theory [25], both curves may be fitted by a two-dimensional interphase controlled process given by Eq. (2) as Fig. 8a and b show.

$$F_{H_2}\alpha\left(\frac{d\alpha}{dt}\right) = Ae^{-E_a/kT}(1-\alpha)^{1/2} \quad (2)$$

where α is the reacted fraction; E_a is the activation energy.

This control process seems to be related to the hexagonal shape of the magnesium crystallites which enhanced a preferred growing direction (along the basal plane). As regards the activation energies (E_a) related to this model, they exhibit values of 130 ± 20 kJ/mol H_2 and 140 ± 10 kJ/mol H_2 for thinner and thicker films respectively. These values are similar to the only reported in the literature [13]. Values also are similar to those obtained in milled magnesium hydride [24] which could indicate the importance of defects such as vacancies and dislocations on the desorption kinetics. In fact, films exhibit much more defects than bulk materials because of the own nanocrystalline nature of films. However, other reasons such as the formation of a Mg–Pd phases at the interface between magnesium and palladium layer should not be disregard in further analysis.

4. Conclusions

It has been shown that capped Pd magnesium hydride films desorb hydrogen under air exposure because of thermodynamic reasons. For instance, films with thickness of 100 nm are completely desorbed after 2000 min. Therefore, for comparison purposes, it is relevant to consider films exposed similar times to air. Moreover, this could be one of the reasons of some discrepancies observed at previous reported results. TDS measurements point out that H-desorption process seems to be controlled by a 2D-interphase control which could be related to preferential hexagonal growing of magnesium crystallites. Finally, magnesium hydride films desorb at 148 °C and desorption temperature and activation energy (135 ± 20 kJ/mol H_2) seems not to be influenced by thickness and/or crystallite size.

Acknowledgements

Authors specially thank to F. Moreno for technical support and CMAM for RBS measurements. This work was financial supported by CAM-UAM project CCG06-UAM/ENE-0508.

References

[1] B. Bogdanovic, K. Bohmhammel, B. Christ, A. Reiser, K. Schlichte, R. Vehlen, U. Wolf, J. Alloys Compd. 288 (1999) 84.
[2] L. Schlapbach, A. Züttel, Nature 414 (2001) 353.
[3] W. Li, C. Li, H. Ma, J. Chen, J. Am. Chem. Soc. 129 (2007) 6170, 21.
[4] B.J. Kooi, G. Palasantzas, J.Th.M. De Hosson, Appl. Phys. Lett. 89 (2006) 161914.
[5] K.-F. Kondo-Zinsou, J.R. Ares, Chem. Mater. 20 (2008) 376.
[6] V. Bérubé, G. Radtke, M. Dresselhaus, G. Chen, Int. J. Energy Res. 31 (2007) 637.
[7] J.N. Huiberts, R. Griessen, J.H. Rector, R.J. Wijngaarden, J.P. Dekker, D.G. de Groot, N.J. Koeman, Nature 380 (1996) 231.
[8] G. Sandrock, S. Suda, L. Schlapbach, Hydrogen Intermetal. Compd. I (1988) 199.
[9] A. Krozer, B. Kasemo, J. Phys.: Condens. Matter (1989) 1533.
[10] K. Higuchi, H. Kajioka, K. Toiyama, H. Fujii, S. Orimo, Y. Kikuchi, J. Alloys Compd. 293–295 (1999) 484.
[11] A. León, E.J. Knystautas, J. Huot, R. Schulz, Thin Solid Films 496 (2006) 683.
[12] R. Domènech-Ferrer, M.G. Sridharan, G. García, F. Pi, J. Rodriguez-Viejo, J. Power Sources 169 (2007), 117-.
[13] R. Checchetto, N. Bazzanella, A. Miotello, R.S. Brusa, A. Zecca, A. Mengucci, J. Appl. Phys. 94 (4) (2004) 1989.
[14] C.W. Ostenfeld, I. Chorkendorff, Surf. Sci. 600 (2006) 1363.
[15] S.J. van der Molen, J.M.J. Kerssermakers, J.H. Rector, N.J. Koeman, B. Dam, R. Griessen, J. Appl. Phys. 86 (1999) 6107.
[16] E. Kótai, Nucl. Instrum. Meth. Phys. Res., Sect. B 85 (1994) 588.
[17] J.F. Fernández, F. Cuevas, C. Sánchez, J. Alloys Compd. 298 (2000) 244.
[18] K. Yamamoto, K. Higuchi, H. Kajioka, H. Sumida, S. Orimo, H. Fujii, J. Alloys Compd. 330–332 (2002) 352.
[19] L.V. Azaroff, Elements of X-ray Crystallography, MacGraw Hill, Tokyo, 1968, p. 549.
[20] C. Donald Ahrens, Essentials of Meteorology, 3rd ed., West Publishing Company, 2001, p. 3.
[21] A.T.M. Van Gogh, S.J. van der Molen, J.W.J. Kerssermakers, N.J. Koeman, R. Griessen, Appl. Phys. Lett. 77 (2000) 815.
[22] C. Nishimura, M. Komaki, M. Amano, J. Alloys Compd. 293–295 (1999) 329.
[23] J. Renner, H.J. Grabke, Z. Metalkd. 69 (1978) 639.
[24] J. Huot, G. Liang, S. Boily, A. Van Neste, E. Shulz, J. Alloys Compd. 293–295 (1999) 495–500.
[25] H. Tanaka, Thermochim. Acta 267 (1995) 29.